Title: Degenerative changes are associated with severity of anterior cruciate ligament injury within the skeletally immature joint

Authors: Danielle Howe[1,2], Jacob D. Thompson[1,2], Stephanie D. Teeter[1], Margaret Easson[1], Olivia Barlow[3], Emily H. Griffith[4], Lauren V. Schnabel[2,5], Jeffrey T. Spang[6], Matthew B. Fisher[1,2,6*]

Affiliations:

[1]Joint Department of Biomedical Engineering, North Carolina State University and the University of North Carolina at Chapel Hill; Raleigh, NC, 27695, USA

[2]Comparative Medicine Institute, North Carolina State University; Raleigh, NC, 27607, USA

[3]Department of Mechanical Engineering, North Carolina State University; Raleigh, NC, 27607, USA

[4]Department of Statistics, North Carolina State University; Raleigh, NC 27695

[5]Department of Clinical Sciences, North Carolina State University; Raleigh, NC, 27695, USA

[6]Department of Orthopaedics, University of North Carolina at Chapel Hill; Chapel Hill, NC, 27599, USA

*Corresponding author. Email: mbfisher@ncsu.edu

One Sentence Summary: Joint degeneration was associated with degree of joint instability after partial and complete ACL injury in a skeletally immature porcine model.

Abstract

Anterior cruciate ligament (ACL) injuries are a major problem in the pediatric and adolescent populations. Some of these injuries extend only partially through the tissue cross-section; yet, there is limited data to inform clinical treatment of such partial tears. In particular, it is unknown how injury severity impacts long-term degenerative changes in the joint. Here, we leverage a skeletally immature preclinical porcine model to evaluate joint biomechanics and degeneration after partial (isolated anteromedial (AM) or posterolateral (PL) bundle) or complete ACL injury. Six months after injury, joint laxity increases were minimal after PL bundle injury, minor after AM bundle injury, and major after ACL injury. Joint degeneration (evaluated in the cartilage and meniscus) was minimal after PL bundle injury, moderate after AM bundle injury, and substantial after ACL injury. With subjects grouped by clinical Lachman grade (indicating the extent of joint destabilization), degeneration was associated with increasing grade, irrespective of injury type. These findings point to the importance of considering joint laxity as a factor when treating young patients, particularly those with partial ACL injuries.

46 **Main Text**

47 Injuries to the anterior cruciate ligament (ACL) of the knee, particularly those occurring
48 in children and adolescents, are a significant clinical and societal concern (*1*). The total number
49 of ACL injuries across all age groups is substantial (200,000-250,000 yearly in the United States
50 alone) (*2, 3*). A specific concern is the 2-4 fold increase in the rate of injury and subsequent
51 surgical treatment in the pediatric population compared to adults (*4-6*).

52 Preventing joint degeneration is a major concern. The natural occurrence of joint
53 degeneration after ACL rupture is well documented in adults (*7*). In the pediatric population,
54 full-thickness ACL tears result in two-fold increases in knee laxity (*8*) and 3-4 times greater risk
55 of developing meniscal and cartilage lesions with delayed surgical intervention (*9*). It is
56 commonly assumed that joint instability after ACL injury is a major factor in subsequent joint
57 degeneration (*10-12*), though the degree of joint instability required to cause degeneration is
58 unknown for skeletally immature patients. Nevertheless, surgical reconstruction is the standard
59 practice to restore joint stability for young, active patients with complete ACL tears (*13*), despite
60 concerns about growth plate disruption.

61 For partial-thickness ACL tears, which account for 10-27% of diagnosed ACL injuries
62 (*14*) and result in a more minor (~30% on average) increase in knee laxity (*15*), the superiority of
63 operative or non-operative treatment to limit degenerative changes is less evidence-based. On
64 one hand, subsequent meniscal and chondral pathologies after non-surgical treatment of partial
65 tears are reported in young patients (*16, 17*). On the other hand, the invasive nature of
66 reconstructive surgery can exacerbate degenerative changes (*18*), and approximately 50% of
67 young patients who undergo ACL reconstruction still develop osteoarthritis after 10 years (*19*).

68 A major complicating factor in determining the best clinical treatment is that not all
69 partial tears are the same. The ACL has two major subregions, the anteromedial (AM) bundle
70 and the posterolateral (PL) bundle, and partial tears can occur in either. Tear location may impact
71 functional outcomes after partial injury, and the results may differ between children and adults.
72 Specifically, a study in adult patients reported similar joint stability after isolated AM and PL
73 bundle injuries (*15*), while a study in pediatric patients reported better outcomes for AM bundle
74 injuries (*20*). Furthermore, in a skeletally immature pig model, the biomechanical function of the
75 AM and PL bundles of the ACL depends on age and sex, such that the AM bundle plays a larger
76 functional role in older versus younger subjects and males versus females (*21, 22*). Since
77 evidence regarding treatment of bundle-specific partial injuries in children and adolescents is
78 sparse, there is a need for further investigation of long-term outcomes and degenerative changes
79 in skeletally immature subjects. Large exploratory studies in humans are challenging to perform
80 in the pediatric patient population. However, the pig is a valuable preclinical model with similar
81 ACL anatomy and function to humans (*23-25*), which can be used to control injury severity and
82 assess functional outcomes and degenerative changes after injury.

83 In the present study, we investigated biomechanics, remodeling, and degeneration in the
84 knee joint after isolated AM bundle, PL bundle, and complete ACL tears in a juvenile porcine
85 model. We hypothesized firstly that partial (AM and PL bundle) tears would result in small
86 levels of instability and degeneration relative to complete ACL tears. Secondly, we hypothesized
87 that remaining soft tissues in the joint would remodel in response to changes in biomechanical
88 loading after ACL injury, such that the degree of remodeling would associate with injury
89 severity. At 6 months after injury, joint laxity showed no change after PL bundle injury, minor
90 increases after AM bundle injury and major increases after ACL injury. Similarly, PL bundle

injury resulted in minimal degeneration, AM bundle injury resulted in moderate degeneration, and complete ACL injury led to substantial degeneration, such that the degree of degenerative changes was associated with joint instability.

Results

Joint kinematics after partial and complete ACL injury

To evaluate the impact of AM and PL bundle tears on knee function and degeneration in skeletally immature subjects, we performed arthroscopic transection and removal of the AM bundle (AM-), PL bundle (PL-) or ACL (ACL-) in juvenile Yorkshire crossbreed pigs and assessed biomechanics and joint health after 24 weeks (Fig. 1a). Joint kinematics were evaluated using a robotic testing system first under applied anterior-posterior (AP) drawer to simulate clinical exams (Fig. 1b-e). AP tibial translation (APTT) was greater in AM- joints (46%, $P<0.0001$) and ACL- joints (195%, $P<0.0001$) compared to contralateral controls, while PL- joints showed no significant difference ($P=0.22$) (Fig. 1c-d). Between injury groups, the inter-limb difference in APTT was significantly different for all comparisons ($P\leq0.0061$) (Fig. 1e). Under applied compression (Fig. 1f-i) (to simulate weight bearing) and varus-valgus moments (Fig. 1j-m) (to simulate rotational loads), anterior tibial translation (ATT) was only greater in ACL- joints compared to contralateral controls (327%, $P=0.0005$) (Fig. 1h), and the interlimb difference in ATT was greater for the ACL- group compared to AM- and PL- groups ($P<0.0001$ for each) (Fig. 1i). Likewise, varus-valgus (VV) rotation was greater in ACL- joints compared to contralateral controls (33%, $P=0.012$) (Fig. 1l), with a larger interlimb difference compared to AM- and PL- groups ($P\leq0.0037$) (Fig. 1m). Sex did not significantly affect kinematics under AP or VV loads, but under compression, ATT was significantly greater in males than females within the AM- group ($P=0.003$) (Supplementary Fig. 1). Overall, PL bundle injury induced minimal

joint instability, AM bundle injury induced moderate joint instability, and complete ACL injury induced major joint instability.

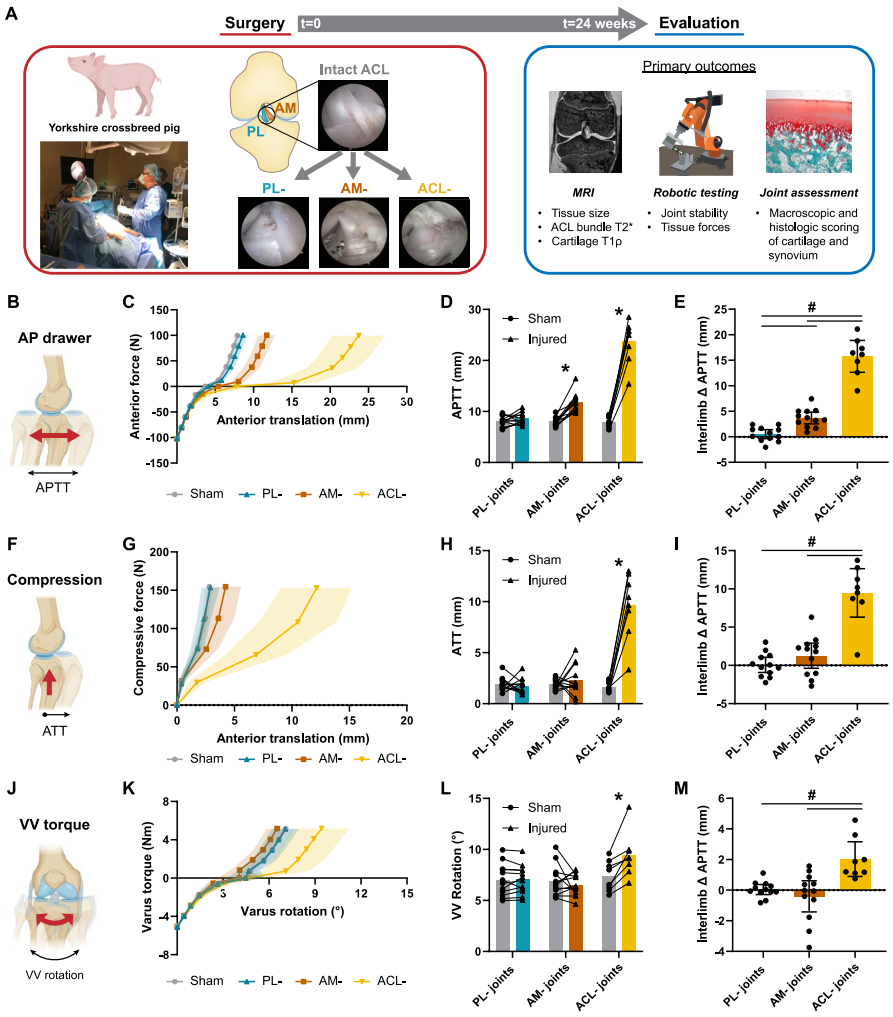

Fig. 1. Biomechanical assessment of porcine joints 6 months after partial and complete ACL transection. a, Schematic of arthroscopic transection of the AM bundle, PL bundle, or entire ACL, followed by evaluation after 24 weeks. b, Diagram of anterior-posterior (AP) loads applied to the tibia. c, Resulting mean force-translation curves. AP tibial translation (APTT) shown as d, absolute values and e, interlimb differences. f, Diagram of compressive load applied to the tibia. g, Resulting mean force-translation curves. Anterior tibial translation (ATT) shown as h, absolute values and i, interlimb differences. j, Diagram of varus-valgus (VV) torques

applied to the tibia. k, Resulting mean torque-rotation curves. VV rotation shown as l, absolute values and m, interlimb differences. Red arrows indicate the direction of the applied load, and black arrows indicate the direction of measured translation (b, f, j). Points and shaded area represent mean ± 95% CI (c, g, k). Lines connect paired joints (d, h, l). Individual data points (n=12 for PL- and AM- groups, n=8 for ACL- group) presented with mean ± 95% CI (e, i, m). * $P<0.05$ between injured and contralateral, from paired t-test with Holm-Sidak correction. #$P<0.05$ between injury type, from one-way ANOVA with Tukey post hoc test.

Subhead 2: Remodeling of the uninjured bundle of the ACL

In partial injury (AM- and PL-) joints, the in-situ force (Fig. 2a) carried by the remaining ACL bundle was greater compared to the corresponding bundle force in contralateral controls under applied anterior drawer ($P\leq0.00019$ for both injury types) (Fig. 2b). However, under joint compression, the remaining bundle force was elevated only for AM- joints ($P=0.0016$) (Fig. 2c). Remaining bundle in-situ force did not differ on average under varus or valgus moments, although considerable specimen-to-specimen variability existed (Supplementary Fig. 2). To assess remodeling of the ACL that may drive functional changes, the cross-sectional area (CSA) of the remaining bundle in injured joints was measured from MRI and compared to the corresponding bundle in contralateral joints (Fig. 2d). The remaining bundle was larger in CSA compared to contralateral controls for PL- joints (AM bundle) by 13% and AM- joints (PL bundle) by 60% ($P\leq0.022$, for both) (Fig. 2e). In addition, bundle collagen organization was assessed through T2* mapping using MRI (Fig. 2f). No differences were found in median T2* value of the remaining bundle in injured joints compared to contralateral controls for either injury group (Fig. 2g).

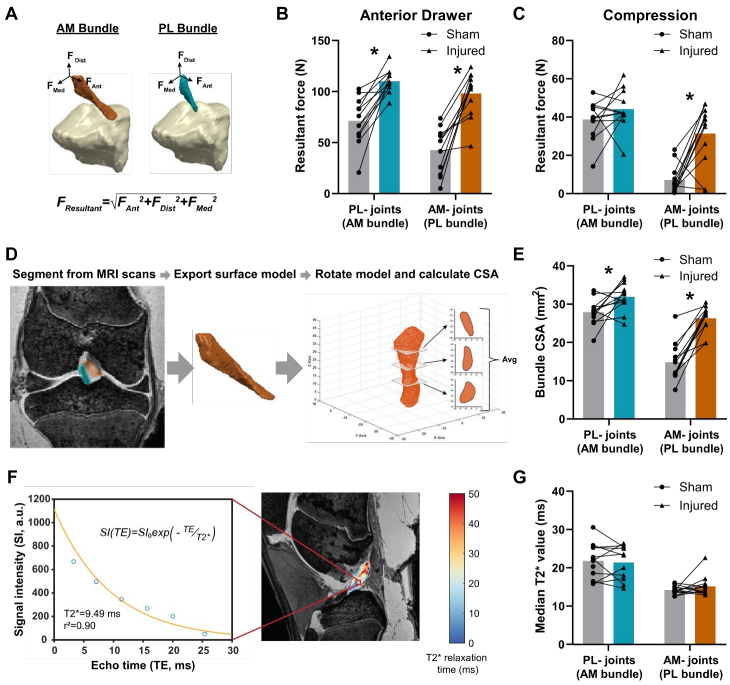

Fig. 2. Remodeling of the remaining bundle after transection of the AM or PL bundle of the ACL. a, Schematic of in-situ bundle forces measured under applied loads. Resultant force in the uninjured bundle under applied b, anterior drawer and c, compression. d, Schematic demonstrating methods used to measure bundle cross-sectional area (CSA) from segmented MRI scans. e, CSA of the uninjured bundle. f, Schematic showing representative sagittal MR image overlaid with the T2* map of the ACL. Plot shows signal intensity at the six measured echo times (blue circles) and fitted monoexponential decay curve (yellow) for a representative voxel. Calculated T2* relaxation time and goodness-of-fit (r^2) shown in graph. g, Median T2* value of the uninjured bundle. Individual data points (n=12 per injury group) presented with mean/median. Lines connect paired joints. *P<0.05 between injured and contralateral, from paired t-test with Holm-Sidak correction.

Subhead 3: Cartilage and synovium degeneration

161 To assess if the type of injury impacted degeneration of articular cartilage in the joint,
162 T1ρ mapping was performed via MRI, and the median T1ρ value was calculated for the medial
163 and lateral femoral and tibial articular cartilage (Fig. 3a). Higher T1ρ values are linked to lower
164 proteoglycan content (*26, 27*). T1ρ values relative to the contralateral control were not
165 significantly elevated in any compartment for the PL- group, but were elevated in the medial
166 femoral and lateral tibial compartments for the AM- group and the lateral femoral and lateral
167 tibial compartments for the ACL- group ($P \leq 0.022$ for all, Fig. 3b-e). Furthermore, the interlimb
168 difference in T1ρ values were significantly greater in the AM- group relative to the PL- group for
169 the medial femoral compartment and in the ACL- group relative to the PL- group for the lateral
170 femoral and lateral tibial compartments ($P \leq 0.012$ for all).
171 Macroscopic articular cartilage damage was scored according to Osteoarthritis Research
172 Society International (OARSI) guidelines (*28*) for the four compartments (Fig. 3f,
173 Supplementary Fig. 3) and summed for a composite joint score. The composite joint scores were
174 significantly elevated only the ACL- group compared to contralateral controls ($P=0.016$ Fig. 3g).
175 Synovium pathology was similarly evaluated through macroscopic scoring, though no significant
176 differences were found between groups (Fig. 3h). A small subset of cartilage was evaluated
177 histologically, but there was high sample-to-sample variability and little discernable differences
178 between injury groups. (Supplementary Fig. 4). Overall, minimal cartilage degradation was
179 observed in PL- joints, and similar increases in cartilage T1ρ values (an early indicator of
180 cartilage degradation) were observed in AM- and ACL- joints; however, macroscopic cartilage
181 degeneration was elevated only in ACL- joints.

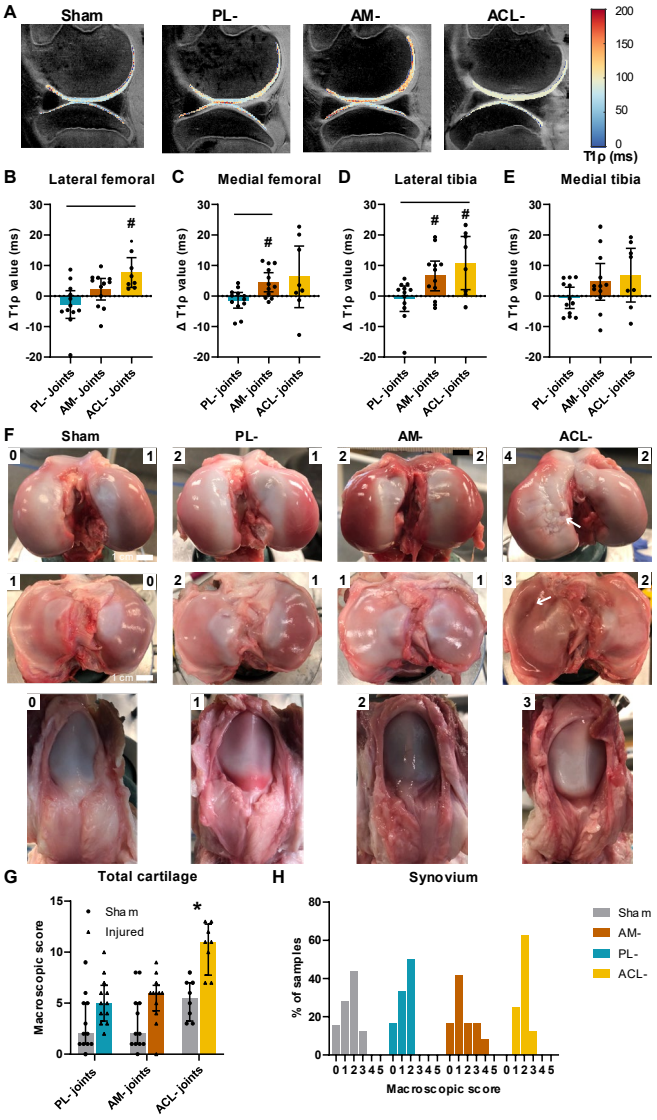

Fig. 3. Cartilage degeneration and synovium inflammation. a, Representative sagittal MR images overlayed with T1ρ maps of articular cartilage. Interlimb differences in T1ρ value for b, lateral femoral, c, medial femoral, d, lateral tibial, and e, medial tibial articular cartilage. #P<0.05 compared to 0 from one sample t-test; bars indicate P<0.05 between injury type, from one-way ANOVA with Tukey post hoc test or Welch ANOVA with Dunnett post hoc test for data sets with unequal variance. f, Representative images of articular cartilage and synovium, with macroscopic scores shown in the corner of each image. White arrows indicate cartilage erosions reaching the subchondral bone. g, Composite macroscopic OARSI scores summed from the four

191 articular cartilage compartments. *P<0.05 compared to contralateral controls from Wilcoxon
192 matched-pairs test. h, Histogram of macroscopic OARSI scores for synovium, presented as a
193 percent of samples for each group. Individual data points (n=12 for PL- and AM- groups, n=8 for
194 ACL- group) presented with mean ± 95% CI (b-e) or median ± IQR (g).
195
196 **Subhead 4: Meniscus degeneration**
197 The biomechanical effect of injury on the menisci of the knee joint was assessed by
198 measuring the in-situ load carried by each tissue under the applied loading conditions. The load
199 carried in the medial meniscus under applied anterior drawer was 33% greater for AM- joints
200 and 3.7-fold greater for ACL- joints compared to contralateral joints (P≤0.029 for each) (Fig.
201 4a), while no significant differences were measured under applied compression (Fig. 4b). The
202 load carried in the lateral meniscus was greater compared to contralateral joints for AM- joints
203 under applied anterior drawer (by 2.7-fold, P=0.008, Fig. 4c) and for ACL- joints under applied
204 compression (by 2.1-fold, P=0.045, Fig. 4d). No differences in meniscal loads were measured in
205 PL- joints relative to contralateral controls. Next, the volume of the menisci were measured from
206 MRI (Fig. 4d) and compared between injured and control joints. The medial and lateral menisci
207 were 11% and 7% larger in AM- joints and 28% and 30% larger in ACL- joints, respectively
208 (P≤0.048 for all, Fig. 4f-g). No changes in meniscal size were measured in PL- joints. For ACL-
209 joints, in addition to the measurable increases in size, the menisci qualitatively developed an
210 oblique shape, and medial menisci developed an unorganized fibrous posterior outgrowth,
211 evident macroscopically and on MRI (Supplementary Fig. 5). Overall, both in-situ loading and
212 volume of the menisci showed no change in PL- joints, moderate increases in AM- joints, and
213 substantial increases in ACL- joints.

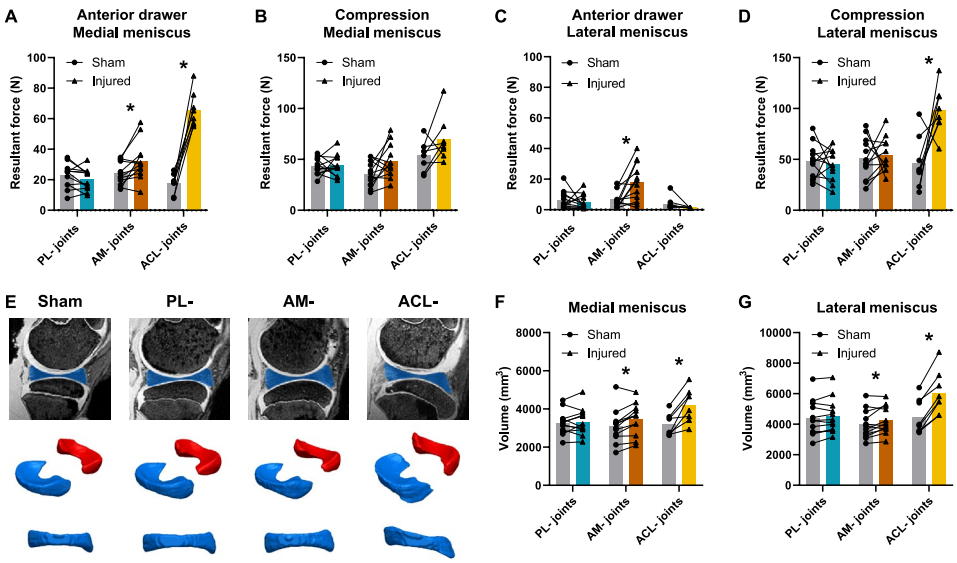

Fig. 4. Changes in meniscal loading and size after partial and complete ACL transection. In-situ forces in the medial meniscus under applied a, anterior drawer and b, axial compression. In-situ forces in the lateral meniscus under applied c, anterior drawer and d, axial compression. e, Representative 3D models of menisci from each injury group, generated from MRI scans. Medial menisci shown in blue, lateral menisci in red. Volume of the f, medial meniscus and g, lateral meniscus. Individual data points (n=12 for PL- and AM- groups, n=8 for ACL- group) presented with mean. Lines connect paired joints. *P<0.05 between injured and contralateral, from paired t-test with Holm-Sidak correction.

Subhead 5: Clinical implications and associations

To investigate whether findings were similar for partial injuries at different ages during skeletal growth, AM and PL bundle injuries were created in adolescent (6-month-old) pigs, and similar results were found (See Supplemental Results and Supplemental Figures 6-7). Using pooled data from both age groups, changes in joint laxity following injury were associated with degenerative changes in the cartilage. Linear regressions were run between interlimb differences

230 in APTT and degenerative outcomes (Fig. 5a-h, Supplementary Fig. 8). Across injury types,
231 significant positive associations existed between interlimb differences in APTT and mean side-
232 to-side differences in T1ρ of the lateral femoral cartilage (r^2=0.16, P=0.0089), lateral meniscus
233 volume (r^2=0.73, P<0.0001), and medial meniscus volume (r^2=0.47, P<0.0001) (Fig. 5a,e,
234 Supplementary Fig. 8). Within injury type, however, there were generally weaker associations
235 for lateral femoral cartilage T1ρ and the interlimb APTT difference (r^2=0.001-0.24) (Fig. 5b-d).
236 For medial meniscus volume, poor associations were also found between the changes in medial
237 meniscus volume and interlimb APTT increases within PL-injured (P=0.58) and ACL-injured
238 (P=0.42) joints. The strongest positive association was found between the medial meniscus
239 volume change and APTT in AM-injured joints, though again with an r^2 value of only 0.26
240 (P=0.046, Fig. 5f-h, Supplementary Fig. 8m-p). Similarly, no significant associations were
241 observed for changes in medial femoral cartilage T1ρ values or lateral meniscus volume and
242 changes in APTT for any injury group (Supplementary Fig. 8e-l).
243 To place the observed degenerative outcomes in a clinically relevant framework,
244 specimens were grouped by equivalent Lachman test grade (Fig. 5i-l, Supplementary Fig. 9),
245 which is a common clinical exam to assess joint stability after ACL injury. Generally, mean side-
246 side differences in lateral femoral cartilage T1ρ values (P=0.048) and medial (P=0.0002)
247 meniscus volume increased progressively for increasing Lachman test grades. Within grade,
248 significant interlimb differences were measured for lateral femoral cartilage T1ρ values only for
249 specimens with Lachman test grades C and D (P≤0.0086), but significant increases in medial
250 meniscus volume were measured for specimens with grade B, C, and D (P≤0.023 for each).
251 Linear regressions were performed within Lachman grades to further investigate associations
252 between joint stability and degeneration (Supplementary Fig. 9), but these were generally weak

(r^2<=0.18). Pooling all injury types, these findings indicate that joint destabilization is positively associated with the extent of joint degradation, but strong associations were not readily apparent within an individual injury type or clinical test grade level.

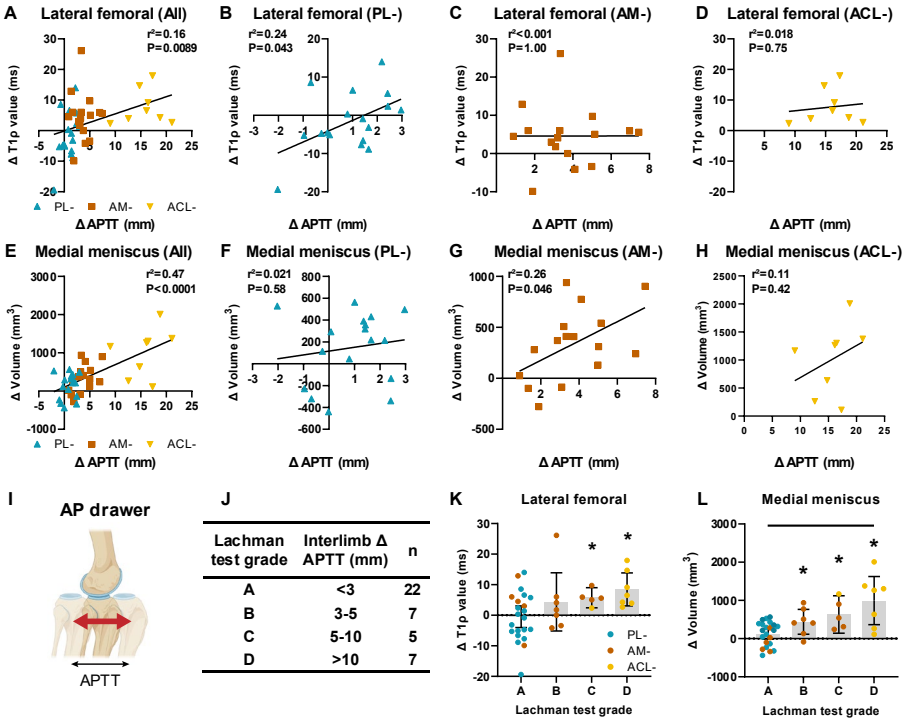

Lachman test grade	Interlimb Δ APTT (mm)	n
A	<3	22
B	3-5	7
C	5-10	5
D	>10	7

Fig. 5. Degenerative outcomes as a function of changes in laxity. a-h, Linear regressions of interlimb difference in APTT versus (a-d) lateral femoral joint cartilage T1ρ and (e-h) medial meniscus volume, across injury groups and separated by PL-, AM-, and ACL-injured joints for pooled juvenile and adolescent pigs. i,j, Lachman test grade from applied anterior-posterior drawer in biomechanical testing used to separate interlimb difference in k, lateral femoral joint cartilage T1ρ and l, medial meniscus volume. *P<0.05 compared to 0 from one sample t-test; bars indicate P<0.05 between injury type, from one-way ANOVA with Tukey post hoc test. Statistical results from linear regression analyses shown in graph. Individual data points (n=17 for PL- and AM- groups, n=8 for ACL- group) presented with mean ± 95% CI (k-l).

267 **D**iscussion

268 There is presently a lack of data to inform clinical treatment of partial ACL injury in young
269 patients, and large exploratory clinical studies are difficult to perform in this patient population.
270 The present study provides a comprehensive analysis of functional and degenerative changes in
271 the knee joint after partial (isolated AM or PL bundle) and complete ACL injury in skeletally
272 immature subjects using a preclinical porcine model and clinically relevant outcome measures.
273 Our results indicate that ACL injury severity (partial or complete) impacts outcomes, and equally
274 importantly, that partial injury location (AM or PL bundle) also impacts outcomes. Across all
275 injury types, the degree of degenerative changes was strongly associated with the extent of joint
276 destabilization. Joint laxity increases were minimal for PL bundle injury, minor for AM bundle
277 injury, and major for ACL injury. In both partial injury cases, the remaining bundle remodeled
278 through an increase in CSA to attempt to restore ACL function and stabilize the knee joint.
279 Cartilage degeneration and meniscal hypertrophy were observed to a minor degree after AM
280 bundle injury and to a major degree after ACL injury, but not after PL bundle injury. Generally,
281 sex did not impact degenerative outcomes in this model.

282 The joint laxity findings in this study are consistent with studies in humans, which report
283 minor (0-6 mm) increases in laxity after partial ACL tears (*8, 15, 18, 20*) compared to major (6-
284 12 mm) increases in laxity after complete ACL tears (*8, 15*). ACL injuries are commonly
285 diagnosed on the field or in the office through physical examination using a Lachman test, which
286 assesses tibial translation under anterior loads, or a pivot shift test, which evaluates tibial
287 subluxation under compressive and rotational loads (*29*). Therefore, the small differences in
288 laxity for partial ACL injuries point to challenges in diagnosis, particularly for PL bundle tears.
289 This is supported by a clinical study in adults which found that 50% of partial tears confirmed

290 through arthroscopy were diagnosed as a false negative using an arthrometer designed to
291 quantify joint laxity (*30*). In the current study, no significant difference in side-to-side laxity was
292 measured under anterior or rotational loads for the PL bundle injury group. In fact, all specimens
293 from the PL bundle injury group fell within the Lachman grade A (indicative of a "normal"
294 joint), suggesting that many of these injuries may go undiagnosed and untreated. Imaging,
295 primarily MRI, can add value as a complementary diagnostic tool in cases where physical
296 examination is inconclusive. Therefore, physical exams paired with MRI appear to be the best
297 current process for diagnosing partial ACL tears, although there remains space for improvement
298 of diagnostic sensitivity and specificity (*15, 31*). Diagnostic accuracy has the potential for
299 improvement through implementing higher resolution MRI protocols or newer sequences
300 capable of better contrast for ligaments (*32*). There also remains the potential for development of
301 new clinical exams which can detect partial injuries.

302 Our functional data is consistent with clinical studies in adults which reported that a
303 greater number of PL bundle injuries were biomechanically functional than AM bundle injuries
304 (*15, 33-35*). Data is less definitive in pediatric patients, since currently only two studies evaluate
305 outcomes after partial injury in young patients (*18, 20*). Kocher et al. found patients with a PL
306 bundle injury were more likely to require a subsequent surgery (*20*), which seems contradictory
307 to findings in this study. However, survivor bias may be a source for this discrepancy. In that
308 study, patients with Lachman grade C or D underwent surgical reconstruction and were not
309 included, which would exclude more AM bundle injuries than PL bundle injury based on our
310 laxity findings. Additionally, it is possible that a greater percentage of AM bundle tears progress
311 to complete ACL tears before receiving treatment. Even without progression to a complete tear,
312 our data shows that degenerative changes can occur after partial ACL injury with joint

instability, suggesting that surgical intervention may be of value even in cases of minor joint instability (Lachman Grade B or higher). Conversely, the lack of degenerative changes in partial ACL injury with no joint instability could provide a rationale for non-operative treatment, allowing more growth to occur prior to surgical intervention if needed.

Our findings are consistent with preclinical in-vivo studies of partial ACL injury as well. A study in skeletally mature sheep found gross and histological cartilage degradation and meniscal damage 40 weeks after AM bundle injury (*36*). Another study in skeletally mature rabbits found histological evidence of meniscal degeneration 8 weeks after both AM and PL bundle injuries (*37*). In adult rabbits, partial ("medial half") and complete ACL injuries led to an increase in joint laxity and histological cartilage damage, and histological scoring was associated with anterior joint stiffness (*38*). Although factors including skeletal maturity, injury location, and time from injury differ between these studies and our study, the consistent findings show that partial ACL injury alone can lead to long-term joint degeneration across different preclinical small and large animal models. Furthermore, our study extends these prior findings to show that degeneration occurs even in the context of skeletally immature joints, despite the potential for higher healing/remodeling capacity.

Several animal studies have tried to associate joint instability and degeneration (*38-40*). However, these studies often involve creating injuries to multiple ligaments (*39*) or stabilizing the joint via surgery (*40*), which limits clinical relevance. Moreover, no study spans the full spectrum of instability corresponding to Lachman grades A through D. This is crucial since patients with grades A or B would be most likely to be treated non-surgically in humans. Additionally, degenerative outcomes are often assessed via histology, which limits their clinical translatability. In our work, we comprehensively compare different types of ACL injury that

336 create a full range of joint instability from Lachman grades A through D, allowing a
337 comprehensive association to degeneration. Additionally, we leverage clinically relevant
338 outcome measures (MRI) that could be used to motivate confirmatory studies in humans (though
339 we also performed traditional gross and histological scoring).

340 Along these lines, the cartilage degeneration that we measured macroscopically and from
341 MRI did not necessarily correspond to one another, particularly in the AM bundle injured group
342 which showed significantly elevated cartilage T1ρ values but little macroscopic cartilage
343 damage. Furthermore, histological scoring of the cartilage was highly variable and did not show
344 clear associations with macroscopic scoring or MRI T1ρ relaxation values. These metrics
345 inherently measure different outcomes, with macroscopic scoring reflecting large structural
346 damage and loss of tissue, T1ρ values reflecting the matrix composition of existing cartilage
347 tissue, and histological scoring reflecting local, 2D structural and cellular damage. While
348 elevated T1ρ values are often used as an early predictor of future degeneration (*41*), macroscopic
349 and histological scoring reflects later-stage structural degeneration. These metrics may capture
350 different phases of degeneration, and we would predict that macroscopic scores for the AM
351 bundle injury group would increase at a longer follow-up timepoint. The difference between
352 outcome metrics also highlights the limited 2D nature of histology (only looking at a thin slice)
353 and suggests that 3D metrics provide a clearer picture of overall cartilage degeneration.

354 In addition to cartilage, changes in the meniscus were also associated with joint
355 instability, suggesting meniscal hypertrophy may also be an early indicator of joint degeneration.
356 This is supported by data from a guineapig model, where meniscal hypertrophy was tied to
357 cartilage damage after ACL injury (*42*). Although little to no data exist regarding meniscal size
358 changes after ACL injury in humans, larger meniscus volume in middle-aged women was tied to

359 later development of structural OA (*43*). While it is common to evaluate meniscal tears after
360 ACL injury, meniscal size, independent of the presence of injury, is often overlooked. However,
361 meniscus size may be an important indicator of overall joint health. Furthermore, meniscus size
362 may be a more repeatable metric across time and would not require specialized MRI sequences,
363 such as T1ρ.

364 The current work has implications for treatment of partial ACL tears, since we showed
365 significant meniscal and chondral pathology after partial ACL injury at the equivalence of a
366 grade B or higher Lachman test. Although we saw differences in outcomes due to injury type, the
367 extent of destabilization may be a better metric as a basis for treatment, since we saw significant
368 associations between cartilage degeneration and joint laxity even within AM bundle injuries. Our
369 results suggest that surgical intervention may be appropriate for patients with Lachman grade B
370 or above, and more likely to be necessary in patients with an AM bundle tear rather than PL
371 bundle tear. Additionally, the increase in remaining bundle CSA with no change in T2* value
372 indicates that viable tissue capable of functional remodeling can remain after a partial ACL
373 injury. This points to advantages in surgical techniques which preserve the intact tissue. Single
374 bundle augmentation techniques which repair or reconstruct only the injured bundle are
375 relatively new but gaining in popularity (*44-48*). These techniques have the advantage of
376 preserving the functional remaining tissue and may cause less donor site morbidity since smaller
377 grafts would be required.

378 This study includes several limitations, including the use of an animal model. While the
379 pig is an established preclinical model for musculoskeletal studies (*23*) and the ACL bundles
380 function similarly between pigs and humans (*24*), there are some differences in knee anatomy
381 (*25*) and physiological loading compared to humans. Furthermore, human patients are prescribed

382 physical therapy and activity restrictions, while we did not attempt to restrict animal activity or
383 acquire metrics for physical activity. Moreover, our evaluation of joint stability does not account
384 for active stabilization provided by the muscles, so it is possible that the joint is more stable in-
385 vivo. Nevertheless, the degenerative changes we detected occurred in the presence of muscle
386 function in-vivo. Additionally, our surgical model of ACL injury does not account for damage to
387 other tissues that may occur during the high impact of a naturally occurring ACL injury.
388 However, our model does isolate the effects of progressive degeneration caused by the loss of
389 joint stability. The injured bundle or entire ACL was removed in our surgical model. This
390 prevents any healing, which has been observed in a limited capacity in clinical cases (*49*). An
391 additional limitation includes the use of contralateral limbs as a control. These may differ from
392 joints in healthy animals due to altered gait or limb compensation after injury of the ipsilateral
393 joint. Lastly, the conclusions in this study are limited to only one timepoint after injury and do
394 not capture the time course of degenerative changes. Future longitudinal studies to assess the
395 progression of the degenerative outcomes would be useful for distinguishing early predictors of
396 degeneration and identifying an ideal window for implementing treatment interventions to
397 prevent degenerative changes.

398 This work fills key gaps in knowledge about degenerative changes after partial and
399 complete ACL injury in skeletally immature subjects. We leverage a large animal model to
400 collect detailed data about joint biomechanics, tissue remodeling, and cartilage degeneration
401 which are not possible to collect in clinical studies. Our data show that the extent of
402 destabilization after an ACL injury may serve as a predictor of degeneration, irrespective of the
403 injury type (partial or complete) or partial injury location (AM or PL bundle). Associations in
404 this study also imply that there may not be a key threshold beyond which degenerative changes

occur, but instead, a continuous gradient where even small increases in laxity can cause minor degeneration. Overall, this study provides a fundamental basis for informing clinical treatments in young patients with partial ACL tears.

Methods

Subhead 1: Study design

The objective of this study was to evaluate the outcomes of partial ACL injury as a function of tear location (AM or PL bundle), with covariates of sex and age, in a skeletally immature surgical porcine model. All animals were bred at the North Carolina State University Swine Educational Unit, and all experimental protocols were approved by the North Carolina State University Institutional Animal Care and Use Committee. Sample sizes were calculated using a power analysis described in the "Statistical analysis" section. A total of 32 juvenile Yorkshire crossbreed pigs (age: 13 ± 1 week, weight: 34 ± 5 kg) underwent unilateral arthroscopic transection of the AM bundle (n=6 female, n=6 male), the PL bundle (n=6 female, n=6 male), or the complete ACL (n=4 female, n=4 male) with a sham operation performed on the contralateral joint. Injury type and injured limb side were randomized. To confirm findings in an older age group, a small subset of 9 adolescent pigs (age: 25 ± 1 week, weight: 129 ± 21 kg) underwent unilateral arthroscopic transection of the AM bundle (n=3 female, n=1 male) or PL bundle (n=4 female, n=1 male). One adolescent animal which was meant to undergo AM bundle transection was excluded due to a pre-existing partial ACL tear to the PL bundle. The endpoint was set at 24 weeks to experimentally evaluate joint biomechanics, cartilage health, and remodeling of soft tissues in the knee joint. Data were collected and analyses were performed in a blinded manner, where possible. No outliers were excluded in the presented data.

428 **Subhead 2: Surgical procedure**

429 Prior to surgery, all pigs were sedated and received analgesics and antimicrobials.
430 Operations were performed arthroscopically (Arthrex Synergy System) under general anesthesia.
431 The knee joints were accessed through medial and lateral parapatellar incisions (~0.5 cm long).
432 The infrapatellar fat pad was partially removed using a 3.5 mm motorized shaver (SabreTooth,
433 Arthrex) to visualize the ACL. A freer elevator was inserted between the AM and PL bundles
434 near the tibial insertion and used to bluntly separate the bundles. A triangle knife (Ectra II Knife
435 4448, Smith & Nephew) was inserted into the separation and (1) turned anteriorly to transect the
436 AM bundle, (2) turned posteriorly to transect the PL bundle, or (3) used to transect the full cross-
437 section of the ACL. The remnant of the transected bundle or complete ligament was debrided
438 using a shaver to ensure loss of function and prevent healing. In the contralateral sham-operated
439 control limb, the infrapatellar pad was similarly partially removed. The ACL bundles were
440 separated with a freer elevator but not transected. Following the operation, skin incisions were
441 suture closed, a local analgesic was administered through subcutaneous injection at the portal
442 sites, and the joint was covered with an antimicrobial adhesive drape. Animals were given
443 analgesics and antimicrobials for 3 days post-operatively. Animals were allowed full weight
444 bearing immediately following surgery and housed in pens with no restriction of movement.
445 After 6 months (23.9 ± 0.3 weeks), all animals were euthanized, and hind limbs were collected.
446 Skin and excess muscle were removed, and knee joints were wrapped in saline-soaked pads and
447 stored at -20 °C.

448 **Subhead 3: Magnetic resonance imaging**

449 Prior to scanning, joints were thawed. Joints were imaged at full extension. Imaging was
450 performed using a Siemens Magnetom Prisma 3T MRI system and a knee coil. Joints were

scanned using a T1ρ fast low-angle shot (FLASH) sequence (FOV: 128x128x84mm, voxel size: 0.4x0.4x1.5mm, FA: 10°, TR: 8.74ms, TE: 4.60ms, spin-lock frequency: 500 Hz, TSL: 0, 10, 20, 30, 40ms) and a T2 susceptibility weighted imaging (SWI) sequence (FOV: 160x160x128mm, voxel size: 0.4x0.4x0.8mm, FA: 12°, TR: 31.0ms, TE: 3.3,7.1,11.4,15.7,20.0,24.4ms). Following scanning, joints were stored at -20 °C for subsequent biomechanical testing. T1ρ and T2* relaxation maps were created by fitting monoexponential decay function on a voxel-by-voxel basis to the 5 spin-lock times and 6 echo times, respectively, using a custom MATLAB script.

Articular cartilage from the medial and lateral condyles of the femur and tibia were manually segmented by a single user from T1ρ images with 0 ms spin-lock time using commercial software (Simpleware ScanIP). Using a MATLAB script, the segmented areas were transposed onto T1ρ relaxation maps described above, and the median T1ρ relaxation time was calculated for each of the four segmented cartilage compartments.

Similarly, the AM bundle, PL bundle, complete ACL, and medial and lateral menisci were manually segmented by a single user from T2* images with 15.7ms echo time. The median T2* relaxation time was calculated for each ACL bundle. Additionally, the volume of each segmented tissue was recorded, and the cross-sectional area (CSA) of the AM and PL bundles and the complete ACL were calculated as previously described (*21, 22*). Briefly, each segmented tissue was exported as a surface mesh, and analyzed using a MATLAB script. Each mesh was rotated such that a line of best fit through the mesh vertices aligned with the z-axis. The CSA was calculated for slices of the mesh in 1 mm increments along the z-axis, then averaged over the middle 50% of slices.

Subhead 4: Biomechanical testing

473 Biomechanics of the knee (stifle) joint were evaluated using a 6 degree-of-freedom
474 (DOF) robotic testing system (KR300 R2500, KRC4, Kuka) equipped with a universal force-
475 moment sensor (Omega160 IP65, ATI Industrial Automation), and integrated through the
476 simVitro software knee module (Cleveland Clinic). To prepare for testing, joints were thawed at
477 room temperature and trimmed to expose the femoral and tibial diaphyses. The femoral head and
478 the distal end of the tibia were removed using a bone saw, then bones were fixed using
479 fiberglass-reinforced epoxy (Everglass, Evercoat) in molds designed to fit in custom clamps for
480 testing. Joints were again stored at -20 °C and thawed at room temperature one day prior to robot
481 testing.

482 The femoral end of the joint was fixed to a rigid testing platform, while the tibial end was
483 fixed to the robotic system at 40° of flexion. A 3D digitizer (G2X MicroScribe) was used to
484 determine an anatomic coordinate system. Joints were sprayed with saline and lightly wrapped in
485 a pad throughout testing to maintain hydration. A passive flexion path was determined by flexing
486 the joint from 40° to 90° while minimizing forces/moments in the remaining 5 DOFs. Then,
487 loads/torques were separately applied to the tibia in the anterior-posterior (AP) (100 N), proximal
488 (axial compression, 140 N), and VV (5 Nm) directions/rotations at 60° of joint flexion while
489 recording kinematic paths. Kinematics were then replayed while recording forces. Next, the joint
490 capsule was removed, and kinematics were replayed while recording forces. The difference in
491 forces measured between the intact and capsule-deficient condition was calculated as the force
492 carried by the joint capsule, by the principle of superposition (*50*). This process was repeated
493 after transection of the AM bundle (or any remnant), PL bundle (or any remnant), MCL, LCL,
494 PCL, medial meniscus, lateral meniscus, medial femoral condyle, and lateral femoral condyle.
495 Joint laxity was measured by anterior-posterior tibial translation (APTT) under AP drawer,

496 anterior tibial translation (ATT) under axial compression, and VV rotation under VV moments.
497 Load-transformation curves were plotted for each loading condition using data points collected at
498 intervals of 20% of the maximum applied load.

499 **Subhead 5: Macroscopic scoring**

500 During robotic testing and tissue dissection, gross images were taken of the synovium
501 following joint capsule dissection, as well as the femoral and tibial articular cartilage, following
502 removal of all other tissues, during robotic testing. Synovium and cartilage were macroscopically
503 scored using Osteoarthritis Research Society International (OARSI) guidelines for sheep and
504 goat (*28*). Although are no scoring guidelines for pigs, this scoring system has been used to
505 evaluate cartilage in previous porcine studies (*51, 52*). Synovial pathology was scored from 0
506 (normal) to 5 (severe), and articular cartilage of medial and lateral condyles of the femur and
507 tibia were scored from 0 (normal) to 4 (large erosions down to subchondral bone) by two blinded
508 reviewers. Disagreements between users were re-examined to determine a consensus. Scores
509 from the four cartilage compartments were added to give a total joint score.

510 **Subhead 6: Histological analyses**

511 Immediately following robotic testing, 5 mm coronal slabs were cut from the lateral
512 femoral condyle (1.5-2 cm from the femoral notch apex) and lateral tibial plateau (1.5-2 cm
513 anterior to the posterior boundary of the tibial plateau) using a bone saw. Samples were fixed in
514 4% paraformaldehyde solution at 4°C for 72 hours, then decalcified in Formical-2000 for 17
515 days. Samples were trimmed to 2-3mm in thickness and embedded in paraffin. 8 μm sections
516 were taken from each sample and stained with safranin-O/fast-green. Whole sections were
517 imaged at 4x magnification using an Olympus IX73 microscope with CellSens software. Two

518 blinded reviewers scored samples adapted from OARSI guidelines (*53*) in the following
519 categories: matrix staining, fibrillation, and focal cell loss.

520 **Subhead 7: Statistical analyses**

521 Sample sizes were determined using a power analysis based on prior work that
522 demonstrated the ability of transection of the AM bundle and ACL in cadaveric joints to generate
523 different levels of initial joint instability (*54*). Using an overall α level of 0.05 (accounting for
524 multiple comparisons), a power of 0.8, and an effect size of 1.5 for the AM- group, a sample size
525 of n=12 was selected to measure a difference between injured and sham-operated joints. For
526 complete loss of ACL function, much larger effect sizes are expected (>3), so a sample size of
527 n=8 was used for this group.

528 Normality of all data sets was confirmed using Shapiro-Wilk test, and equal variance
529 between data sets was tested using Brown-Forsythe test. Joint kinematics, tissue forces under
530 applied loads, tissue size metrics, and bundle T2* values were compared between injured and
531 sham-operated joints using paired t-tests with Holm-Sidak's correction for multiple comparisons.
532 Outliers were removed from lateral meniscus forces under anterior drawer using the iterative
533 Grubbs' method with an alpha of 0.05. Interlimb differences in joint kinematics, cartilage T1ρ,
534 and meniscal volumes were compared between injury types and ages of injury using a two-way
535 ANOVA with Holm-Sidak post hoc comparison. Interlimb differences in macroscopic and
536 histologic cartilage scores were compared between AM-injury and PL-injured joints in juvenile
537 and adolescent pigs with Mann-Whitney tests. For data sets with unequal variance, Welch
538 ANOVA with Dunnett post hoc comparison was used. To evaluate clinically relevant outcomes,
539 samples were grouped into equivalent Lachman test grades according to IKDC guidelines (A: <3
540 mm, B: 3-5 mm, C: 5-10 mm, D: >10 mm) (*55*), based on joint translations under AP drawer.

Interlimb differences in cartilage T1ρ, macroscopic cartilage scores, and meniscal volume were compared between Lachman grades using one-way ANOVA and compared to zero with one sample t-test. Associations were assessed between interlimb differences in APTT and interlimb differences in cartilage T1ρ and meniscal volume using linear regression across all injury types and within injury types. All statistical analyses were performed in Prism (GraphPad), with overall significance set at $\alpha=0.05$ for all analyses with corrections for multiple comparisons done as needed. Adjusted P values are reported. Data presented as mean ± 95% CI, unless stated otherwise, and data are reported in supplemental material.

Data availability

The main data supporting the results in this study are available within the paper and its Supplementary Information.

References

1. G. Kolata, If You Tear a Knee Ligament, Arthritis Is Likely to Follow in 10 YearsN. Y. Times (2017) (available at https://www.nytimes.com/2017/11/06/health/arthritis-risk-acl.html).

2. T. L. Sanders, H. Maradit Kremers, A. J. Bryan, D. R. Larson, D. L. Dahm, B. A. Levy, M. J. Stuart, A. J. Krych, Incidence of Anterior Cruciate Ligament Tears and Reconstruction: A 21-Year Population-Based Study. *Am J Sports Med* **44**, 1502-1507 (2016).

3. N. A. Mall, P. N. Chalmers, M. Moric, M. J. Tanaka, B. J. Cole, B. R. Bach, Jr., G. A. Paletta, Jr., Incidence and trends of anterior cruciate ligament reconstruction in the United States. *Am J Sports Med* **42**, 2363-2370 (2014).

4. B. C. Werner, S. Yang, A. M. Looney, F. W. Gwathmey, Jr., Trends in Pediatric and Adolescent Anterior Cruciate Ligament Injury and Reconstruction. *J Pediatr Orthop* **36**, 447-452 (2016).

5. D. Zbrojkiewicz, C. Vertullo, J. E. Grayson, Increasing rates of anterior cruciate ligament reconstruction in young Australians, 2000-2015. *Med J Aust* **208**, 354-358 (2018).

6. E. R. Dodwell, L. E. Lamont, D. W. Green, T. J. Pan, R. G. Marx, S. Lyman, 20 years of pediatric anterior cruciate ligament reconstruction in New York State. *Am J Sports Med* **42**, 675-680 (2014).

7. D. Dare, S. Rodeo, Mechanisms of post-traumatic osteoarthritis after ACL injury. *Curr Rheumatol Rep* **16**, 448 (2014).

8. D. M. Daniel, M. L. Stone, R. Sachs, L. Malcom, Instrumented measurement of anterior knee laxity in patients with acute anterior cruciate ligament disruption. *Am J Sports Med* **13**, 401-407 (1985).

9. I. Kawashima, H. Hiraiwa, S. Ishizuka, R. Kawai, Y. Kusaka, K. Ohtomo, T. Tsukahara, Incidence of Medial and Lateral Meniscal Tears After Delayed Anterior Cruciate Ligament Reconstruction in Pediatric Patients. *Orthop J Sports Med* **8**, 2325967120964603 (2020).

10. P. Neuman, I. Kostogiannis, T. Friden, H. Roos, L. E. Dahlberg, M. Englund, Knee laxity after complete anterior cruciate ligament tear: a prospective study over 15 years. *Scand J Med Sci Sports* **22**, 156-163 (2012).

11. P. D. Fabricant, M. S. Kocher, Management of ACL Injuries in Children and Adolescents. *J Bone Joint Surg Am* **99**, 600-612 (2017).

12. H. Mizuta, K. Kubota, M. Shiraishi, Y. Otsuka, N. Nagamoto, K. Takagi, The conservative treatment of complete tears of the anterior cruciate ligament in skeletally immature patients. *J Bone Joint Surg Br* **77**, 890-894 (1995).

13. C. L. Ardern, G. Ekas, H. Grindem, H. Moksnes, A. Anderson, F. Chotel, M. Cohen, M. Forssblad, T. J. Ganley, J. A. Feller, J. Karlsson, M. S. Kocher, R. F. LaPrade, M. McNamee, B. Mandelbaum, L. Micheli, N. Mohtadi, B. Reider, J. Roe, R. Seil, R. Siebold, H. J. Silvers-Granelli, T. Soligard, E. Witvrouw, L. Engebretsen, 2018 International Olympic Committee consensus statement on prevention, diagnosis and management of paediatric anterior cruciate ligament (ACL) injuries. *Knee Surg Sports Traumatol Arthrosc*, (2018).

14. P. Colombet, D. Dejour, J. C. Panisset, R. Siebold, S. French Arthroscopy, Current concept of partial anterior cruciate ligament ruptures. *Orthop Traumatol Surg Res* **96**, S109-118 (2010).

15. D. Dejour, P. G. Ntagiopoulos, P. R. Saggin, J. C. Panisset, The diagnostic value of clinical tests, magnetic resonance imaging, and instrumented laxity in the differentiation of complete versus partial anterior cruciate ligament tears. *Arthroscopy* **29**, 491-499 (2013).

604 16. E. R. Hunt, C. A. Jacobs, C. E. Conley, M. L. Ireland, D. L. Johnson, C. Lattermann,
605 Anterior cruciate ligament reconstruction reinitiates an inflammatory and
606 chondrodegenerative process in the knee joint. *J Orthop Res* **39**, 1281-1288 (2021).

607 17. P. N. Chalmers, N. A. Mall, M. Moric, S. L. Sherman, G. P. Paletta, B. J. Cole, B. R.
608 Bach, Jr., Does ACL reconstruction alter natural history?: A systematic literature review
609 of long-term outcomes. *J Bone Joint Surg Am* **96**, 292-300 (2014).

610 18. J. M. Fayard, B. Sonnery-Cottet, G. Vrgoc, P. O'Loughlin, G. D. de Mont Marin, B.
611 Freychet, T. D. Vieira, M. Thaunat, Incidence and Risk Factors for a Partial Anterior
612 Cruciate Ligament Tear Progressing to a Complete Tear After Nonoperative Treatment in
613 Patients Younger Than 30 Years. *Orthop J Sports Med* **7**, 2325967119856624 (2019).

614 19. M. Group, J. S. Everhart, M. H. Jones, S. Yalcin, E. K. Reinke, L. J. Huston, J. T.
615 Andrish, C. L. Cox, D. C. Flanigan, C. C. Kaeding, R. A. Magnussen, N. Obuchowski, R.
616 D. Parker, A. D. Pedroza, R. A. Sanders, C. S. Winalski, K. P. Spindler, The Clinical
617 Radiographic Incidence of Posttraumatic Osteoarthritis 10 Years After Anterior Cruciate
618 Ligament Reconstruction: Data From the MOON Nested Cohort. *Am J Sports Med* **49**,
619 1251-1261 (2021).

620 20. M. S. Kocher, L. J. Micheli, D. Zurakowski, A. Luke, Partial tears of the anterior cruciate
621 ligament in children and adolescents. *Am J Sports Med* **30**, 697-703 (2002).

622 21. S. G. Cone, E. P. Lambeth, H. Ru, L. A. Fordham, J. A. Piedrahita, J. T. Spang, M. B.
623 Fisher, Biomechanical Function and Size of the Anteromedial and Posterolateral Bundles
624 of the ACL Change Differently with Skeletal Growth in the Pig Model. *Clin Orthop*
625 *Relat Res* **477**, 2161-2174 (2019).

626 22. D. Howe, S. G. Cone, J. A. Piedrahita, B. Collins, L. A. Fordham, E. H. Griffith, J. T.
627 Spang, M. B. Fisher, Sex-specific biomechanics and morphology of the anterior cruciate
628 ligament during skeletal growth in a porcine model. *J Orthop Res*, (2021).

629 23. S. G. Cone, P. B. Warren, M. B. Fisher, Rise of the Pigs: Utilization of the Porcine Model
630 to Study Musculoskeletal Biomechanics and Tissue Engineering During Skeletal Growth.
631 *Tissue Eng Part C Methods* **23**, 763-780 (2017).

632 24. J. W. Xerogeanes, R. J. Fox, Y. Takeda, H. S. Kim, Y. Ishibashi, G. J. Carlin, S. L. Woo,
633 A functional comparison of animal anterior cruciate ligament models to the human
634 anterior cruciate ligament. *Ann Biomed Eng* **26**, 345-352 (1998).

635 25. B. L. Proffen, M. McElfresh, B. C. Fleming, M. M. Murray, A comparative anatomical
636 study of the human knee and six animal species. *Knee* **19**, 493-499 (2012).

637 26. R. R. Regatte, S. V. Akella, A. J. Wheaton, G. Lech, A. Borthakur, J. B. Kneeland, R.
638 Reddy, 3D-T1rho-relaxation mapping of articular cartilage: in vivo assessment of early
639 degenerative changes in symptomatic osteoarthritic subjects. *Acad Radiol* **11**, 741-749
640 (2004).

641 27. S. V. Akella, R. R. Regatte, A. J. Gougoutas, A. Borthakur, E. M. Shapiro, J. B.
642 Kneeland, J. S. Leigh, R. Reddy, Proteoglycan-induced changes in T1rho-relaxation of
643 articular cartilage at 4T. *Magn Reson Med* **46**, 419-423 (2001).

644 28. C. B. Little, M. M. Smith, M. A. Cake, R. A. Read, M. J. Murphy, F. P. Barry, The
645 OARSI histopathology initiative - recommendations for histological assessments of
646 osteoarthritis in sheep and goats. *Osteoarthritis Cartilage* **18 Suppl 3**, S80-92 (2010).

647 29. V. Musahl, I. D. Engler, E. M. Nazzal, J. F. Dalton, G. A. Lucidi, J. D. Hughes, S.
648 Zaffagnini, F. Della Villa, J. J. Irrgang, F. H. Fu, J. Karlsson, Current trends in the
649 anterior cruciate ligament part II: evaluation, surgical technique, prevention, and
650 rehabilitation. *Knee Surg Sports Traumatol Arthrosc* **30**, 34-51 (2022).

651 30. J. Isberg, E. Faxen, S. Brandsson, B. I. Eriksson, J. Karrholm, J. Karlsson, KT-1000
652 records smaller side-to-side differences than radiostereometric analysis before and after
653 an ACL reconstruction. *Knee Surg Sports Traumatol Arthrosc* **14**, 529-535 (2006).

654 31. P. Van Dyck, E. De Smet, J. Veryser, V. Lambrecht, J. L. Gielen, F. M. Vanhoenacker,
655 L. Dossche, P. M. Parizel, Partial tear of the anterior cruciate ligament of the knee: injury
656 patterns on MR imaging. *Knee Surg Sports Traumatol Arthrosc* **20**, 256-261 (2012).

657 32. N. C. Nacey, M. G. Geeslin, G. W. Miller, J. L. Pierce, Magnetic resonance imaging of
658 the knee: An overview and update of conventional and state of the art imaging. *J Magn*
659 *Reson Imaging* **45**, 1257-1275 (2017).

660 33. P. S. Christel, U. Akgun, T. Yasar, M. Karahan, B. Demirel, The contribution of each
661 anterior cruciate ligament bundle to the Lachman test: a cadaver investigation. *J Bone*
662 *Joint Surg Br* **94**, 68-74 (2012).

663 34. R. L. Hole, D. M. Lintner, E. Kamaric, J. B. Moseley, Increased tibial translation after
664 partial sectioning of the anterior cruciate ligament. The posterolateral bundle. *Am J*
665 *Sports Med* **24**, 556-560 (1996).

666 35. R. Siebold, F. H. Fu, Assessment and augmentation of symptomatic anteromedial or
667 posterolateral bundle tears of the anterior cruciate ligament. *Arthroscopy* **24**, 1289-1298
668 (2008).

669 36. K. I. Barton, B. J. Heard, J. L. Sevick, C. R. Martin, S. M. M. Shekarforoush, M. Chung,
670 Y. Achari, C. B. Frank, N. G. Shrive, D. A. Hart, Posttraumatic Osteoarthritis
671 Development and Progression in an Ovine Model of Partial Anterior Cruciate Ligament
672 Transection and Effect of Repeated Intra-articular Methylprednisolone Acetate Injections
673 on Early Disease. *Am J Sports Med* **46**, 1596-1605 (2018).

674 37. D. Wang, Z. Wang, M. Li, S. Xu, The underlying mechanism of partial anterior cruciate
675 ligament injuries to the meniscus degeneration of knee joint in rabbit models. *J Orthop*
676 *Surg Res* **15**, 428 (2020).

677 38. Y. Tochigi, T. Vaseenon, A. D. Heiner, D. C. Fredericks, J. A. Martin, M. J. Rudert, S. L.
678 Hillis, T. D. Brown, T. O. McKinley, Instability dependency of osteoarthritis
679 development in a rabbit model of graded anterior cruciate ligament transection. *J Bone*
680 *Joint Surg Am* **93**, 640-647 (2011).

681 39. C. B. Frank, J. E. Beveridge, K. D. Huebner, B. J. Heard, J. E. Tapper, E. J. O'Brien, N.
682 G. Shrive, Complete ACL/MCL deficiency induces variable degrees of instability in
683 sheep with specific kinematic abnormalities correlating with degrees of early
684 osteoarthritis. *J Orthop Res* **30**, 384-392 (2012).

685 40. K. Murata, N. Kanemura, T. Kokubun, T. Fujino, Y. Morishita, K. Onitsuka, S. Fujiwara,
686 A. Nakajima, D. Shimizu, K. Takayanagi, Controlling joint instability delays the
687 degeneration of articular cartilage in a rat model. *Osteoarthritis Cartilage* **25**, 297-308
688 (2017).

689 41. H. F. Atkinson, T. B. Birmingham, R. F. Moyer, D. Yacoub, L. E. Kanko, D. M. Bryant,
690 J. D. Thiessen, R. T. Thompson, MRI T2 and T1rho relaxation in patients at risk for knee
691 osteoarthritis: a systematic review and meta-analysis. *BMC Musculoskelet Disord* **20**, 182
692 (2019).

693 42. G. Du, H. Zhan, D. Ding, S. Wang, X. Wei, F. Wei, J. Zhang, B. Bilgen, A. M. Reginato,
694 B. C. Fleming, J. Deng, L. Wei, Abnormal Mechanical Loading Induces Cartilage
695 Degeneration by Accelerating Meniscus Hypertrophy and Mineralization After ACL
696 Injuries In Vivo. *Am J Sports Med* **44**, 652-663 (2016).

697 43. D. Xu, J. van der Voet, J. H. Waarsing, E. H. Oei, S. Klein, M. Englund, F. Zhang, S.
698 Bierma-Zeinstra, J. Runhaar, Are changes in meniscus volume and extrusion associated
699 to knee osteoarthritis development? A structural equation model. *Osteoarthritis Cartilage*
700 **29**, 1426-1431 (2021).

701 44. B. Sonnery-Cottet, R. Zayni, J. Conteduca, P. Archbold, T. Prost, Y. Carrillon, J. Clechet,
702 M. Thaunat, Posterolateral Bundle Reconstruction With Anteromedial Bundle Remnant
703 Preservation in ACL Tears: Clinical and MRI Evaluation of 39 Patients With 24-Month
704 Follow-up. *Orthop J Sports Med* **1**, 2325967113501624 (2013).

705 45. N. Shohat, D. Lindner, E. Tamir, Y. Beer, G. Agar, Prospective Comparison between
706 Remnant-Preserving Augmentation and Double-Bundle Reconstruction in Anterior
707 Cruciate Ligament Tears. *Isr Med Assoc J* **19**, 355-359 (2017).

708 46. A. M. Gipsman, N. Trasolini, G. F. R. Hatch, 3rd, Primary Anterior Cruciate Ligament
709 Single-Bundle Repair With Augmentation for a Partial Anterior Cruciate Ligament Tear.
710 *Arthrosc Tech* **7**, e367-e372 (2018).

711 47. G. Y. Ahn, T. H. Lee, K. J. Lee, S. Woo, Comparison of clinical outcomes and second-
712 look arthroscopic evaluations between anterior cruciate ligament anteromedial bundle
713 augmentation and single-bundle anterior cruciate ligament reconstruction. *Knee Surg*
714 *Relat Res* **32**, 45 (2020).

48. T. Tajima, N. Yamaguchi, Y. Morita, T. Yokoe, M. Nagasawa, T. Ota, S. Kawagoe, Y. Nakamura, E. Chosa, Remnant-Preserved Single-Bundle Anterior Cruciate Ligament Augmentation in Multi-ligamentous Knee Reconstruction. *J Knee Surg*, (2022).

49. E. H. Crain, D. C. Fithian, E. W. Paxton, W. F. Luetzow, Variation in anterior cruciate ligament scar pattern: does the scar pattern affect anterior laxity in anterior cruciate ligament-deficient knees? *Arthroscopy* **21**, 19-24 (2005).

50. G. A. Livesay, H. Fujie, S. Kashiwaguchi, D. A. Morrow, F. H. Fu, S. L. Woo, Determination of the in situ forces and force distribution within the human anterior cruciate ligament. *Ann Biomed Eng* **23**, 467-474 (1995).

51. N. P. Karamchedu, M. M. Murray, J. T. Sieker, B. L. Proffen, G. Portilla, M. Q. Costa, J. Molino, B. C. Fleming, Bridge-Enhanced Anterior Cruciate Ligament Repair Leads to Greater Limb Asymmetry and Less Cartilage Damage Than Untreated ACL Transection or ACL Reconstruction in the Porcine Model. *Am J Sports Med* **49**, 667-674 (2021).

52. M. P. Pinette, J. Molino, B. L. Proffen, M. M. Murray, B. C. Fleming, Effects of Male and Female Sex on the Development of Posttraumatic Osteoarthritis in the Porcine Knee After Anterior Cruciate Ligament Surgery. *Am J Sports Med*, 3635465221102118 (2022).

53. C. W. McIlwraith, D. D. Frisbie, C. E. Kawcak, C. J. Fuller, M. Hurtig, A. Cruz, The OARSI histopathology initiative - recommendations for histological assessments of osteoarthritis in the horse. *Osteoarthritis Cartilage* **18 Suppl 3**, S93-105 (2010).

54. D. Howe, S. G. Cone, J. A. Piedrahita, J. T. Spang, M. B. Fisher, Age and Sex-Specific Joint Biomechanics in Response to Partial and Complete ACL Injury in the Porcine Model. *J Athl Train*, (2021).

55. E. P. Mulligan, D. Q. McGuffie, K. Coyner, M. Khazzam, The reliability and diagnostic accuracy of assessing the translation endpoint during the lachman test. *Int J Sports Phys Ther* **10**, 52-61 (2015).

Acknowledgments

We would like to thank Laboratory Animal Resources (NC State) and the Biomedical Research Imaging Center (UNC-CH) for their contributions to this work. This work was supported by the National Institutes of Health (NIH) grants F31AR077997 and R01AR071985, and the National Science Foundation (NSF) grant DGE-1746939.

Author contributions

D.H., L.V.S., J.T.S. and M.B.F. conceptualized the work. D.H., J.D.T., S.D.T., M.E., E.H.G., L.V.S., J.T.S. and M.B.F. designed the methodology. D.H., J.D.T., S.D.T., M.E., O.B., L.V.S., J.T.S. and M.B.F. investigated the work. Formal analysis was carried out by D.H., J.D.T., S.D.T., M.E., E.H.G. and M.B.F. Data was curated by D.H., J.D.T., S.D.T., and M.E. D.H., J.D.T., M.E. and M.B.F. created the figures for this work. Funding was acquired by D.H., J.D.T., L.V.S., J.T.S. and M.B.F., and the project administration was D.H. and M.B.F. with M.B.F. providing supervision. D.H. wrote the original draft and all authors reviewed and edited the paper.

Competing interests

Authors declare that they have no competing interests.

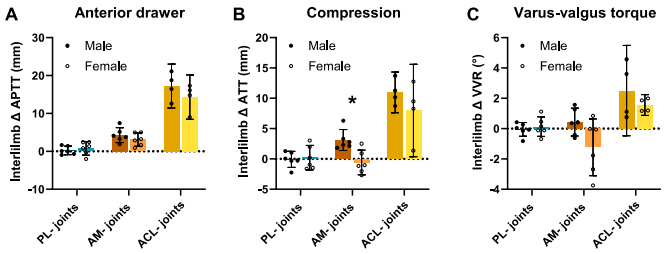

Supplementary Fig. 1. Sex-specific biomechanical outcomes. Interlimb differences in (A) anterior-posterior tibial translation (APTT) under applied AP drawer, (B) anterior tibial translation (ATT) under applied axial compression, and (C) varus-valgus (VV) rotation under applied VV moments. Individual data points presented with mean ± 95% CI. * P<0.05 between male and female, from one-way ANOVA with Tukey post hoc test.

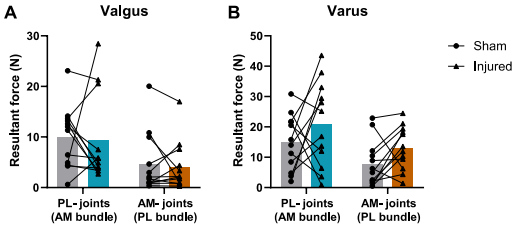

Supplementary Fig. 2. In-situ bundle forces under rotational loads. Resultant force in the uninjured bundle under applied (A) valgus moments and (B) varus moments. Lines connect paired joints. Individual data points presented with mean.

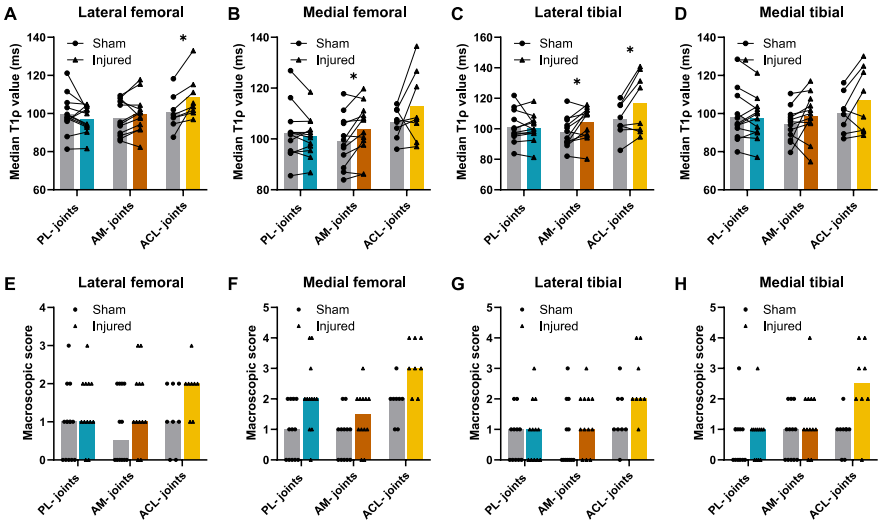

Supplementary Fig. 3. T1ρ values and macroscopic scores of cartilage compartments. T1ρ values of the (A) lateral femoral, (B) lateral tibial, (C) medial femoral, and (D) medial tibial cartilage compartments. Macroscopic

OARSI score of the (E) lateral femoral, (F) lateral tibial, (G) medial femoral, and (H) medial tibial cartilage compartments. Individual data points presented with mean with lines connecting paired joints (A-D) or median ± IQR (E-H). *P<0.05 between injured and contralateral, from paired t-test with Holm-Sidak correction.

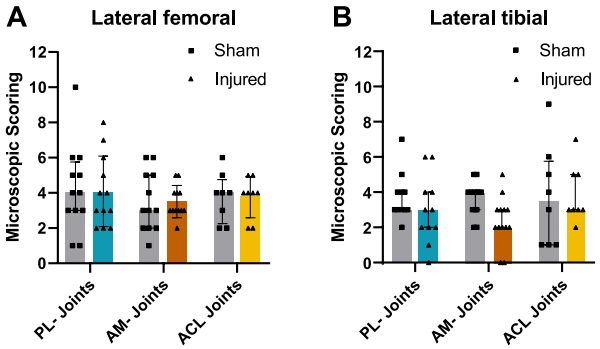

Supplementary Fig. 4. Histological scoring of lateral femoral and tibial cartilage samples stained with safranin-O and fast green. Representative images taken from samples in sham-operated, PL-, AM-, and ACL- joints. Summed composite histological scores shown for the (A) lateral femoral cartilage and (B) lateral tibial cartilage. Individual data points presented with median ± IQR.

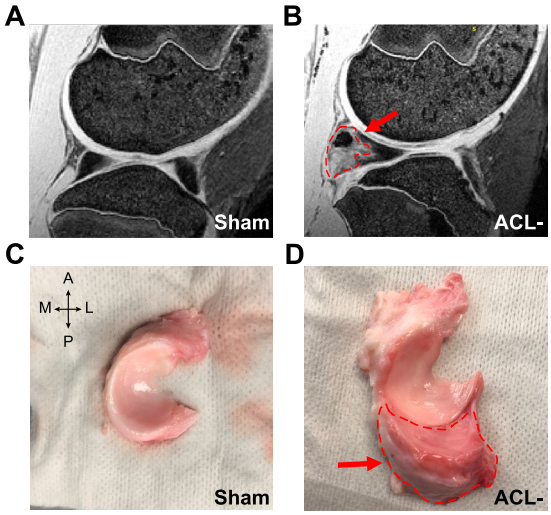

Supplementary Fig. 5. MRI and macroscopic images of medial menisci from sham-operated and ACL- joints. (A,C) Sham-operated control shows normal anatomy of the medial meniscus, where (B,D) red dotted lines and arrows indicate degenerative, fibrous outgrowth in ACL-injured joints. Anterior-posterior and medial-lateral directions indicated.

787 **Supplementary Results & Discussion: Extension to adolescent animals**

788 To investigate whether findings were similar for partial injuries at different ages during
789 skeletal growth, AM and PL bundle injuries were created in adolescent (6-month-old) pigs. Joint
790 biomechanics, cartilage health, and meniscus volume were evaluated after 24 weeks. Interlimb
791 differences in joint laxity were similarly elevated for AM- joints under AP drawer ($P<0.05$) in
792 both the adolescent and juvenile injury groups, with no significant difference in laxity for the PL-
793 group (Supplementary Fig. 6A, Fig. S6A). Laxity results were also similar between the two age
794 groups under varus-valgus torque and compression for the PL-injured joints (Fig. S6B-C and
795 Fig. 1). Both juvenile and adolescent age groups had similar increases of ~1-2 mm in laxity
796 under compression for AM-injured joints, yet the adolescent group had a statistically significant
797 increase in laxity where the juvenile group did not (Fig. S6B and Fig. 1). For both age groups,
798 lateral and medial femoral cartilage T1ρ values and composite macroscopic cartilage scores
799 appeared similarly elevated in AM- joints but not PL- joints, with the medial femoral cartilage
800 T1ρ having statistically significantly higher ($P<0.05$) T1ρ values for AM-injured joints for both
801 juvenile and adolescent age groups (Fig. 5B-D and Fig. S6F-J). Lastly, the interlimb differences
802 in medial and lateral meniscus volume were elevated ~5-10% after partial injury in adolescent
803 animals similar to juvenile animals (Fig. S6D and E). Although sample size was limited for
804 adolescent animals (n=4-5 per injury type), these data highlight similarities across two age
805 groups, adding confidence to our findings in younger animals with larger sample sizes.
806

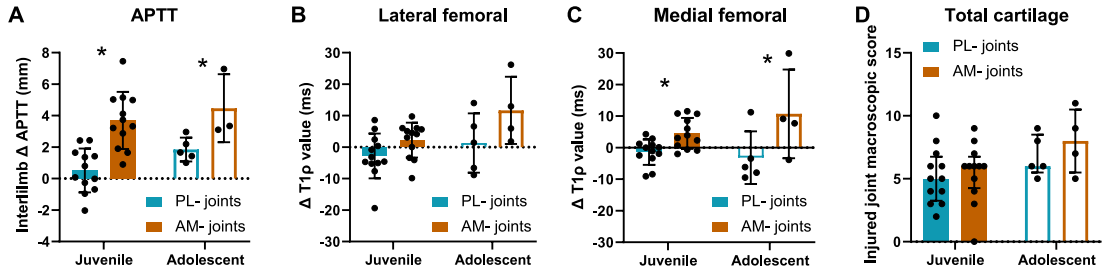

Supplementary Fig. 6. Joint laxity and tissue remodeling after partial ACL injury created in adolescent compared to juvenile pigs. (A) Interlimb differences in APTT under applied AP drawer. (B) Interlimb differences in T1ρ value for lateral femoral articular cartilage and (C) medial femoral articular cartilage. (D) Interlimb differences in macroscopic cartilage. Individual data points (n=5 for PL- and n=4 for AM- adolescent groups, n=12 for PL- and AM- juvenile groups) presented with mean ± 95% CI (A,B,D,E) or median ± IQR (C). *P<0.05 between PL- and AM- injured joints, from two-way ANOVA with Holm-Sidak correction. Multiple comparisons were run using Mann-Whitney test for interlimb differences in macroscopic scoring between PL- and AM- injured joints for juvenile and adolescent animals.

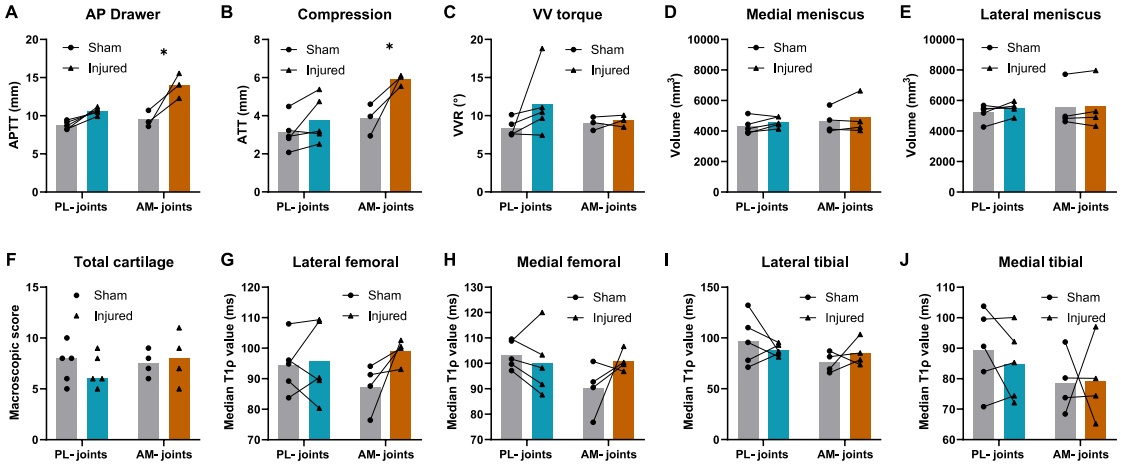

Supplementary Fig. 7. Biomechanical and degenerative outcomes after partial injuries created in adolescent (6 month) pigs. (A) APTT under applied AP drawer, (B) ATT under applied axial compression, and (C) VV rotation under applied VV moments. Volume of the (D) medial meniscus and (E) lateral meniscus. (F) Composite macroscopic OARSI scores summed from the four articular cartilage compartments. T1ρ value for (G) lateral femoral, (H) medial femoral, (I) lateral tibial, and (J) medial tibial articular cartilage. Lines connect paired joints.

824 Individual data points (n=5 for PL- and n=4 for AM- groups) presented with mean. *P<0.05 between injured and

825 contralateral, from paired t-test with Holm-Sidak correction.

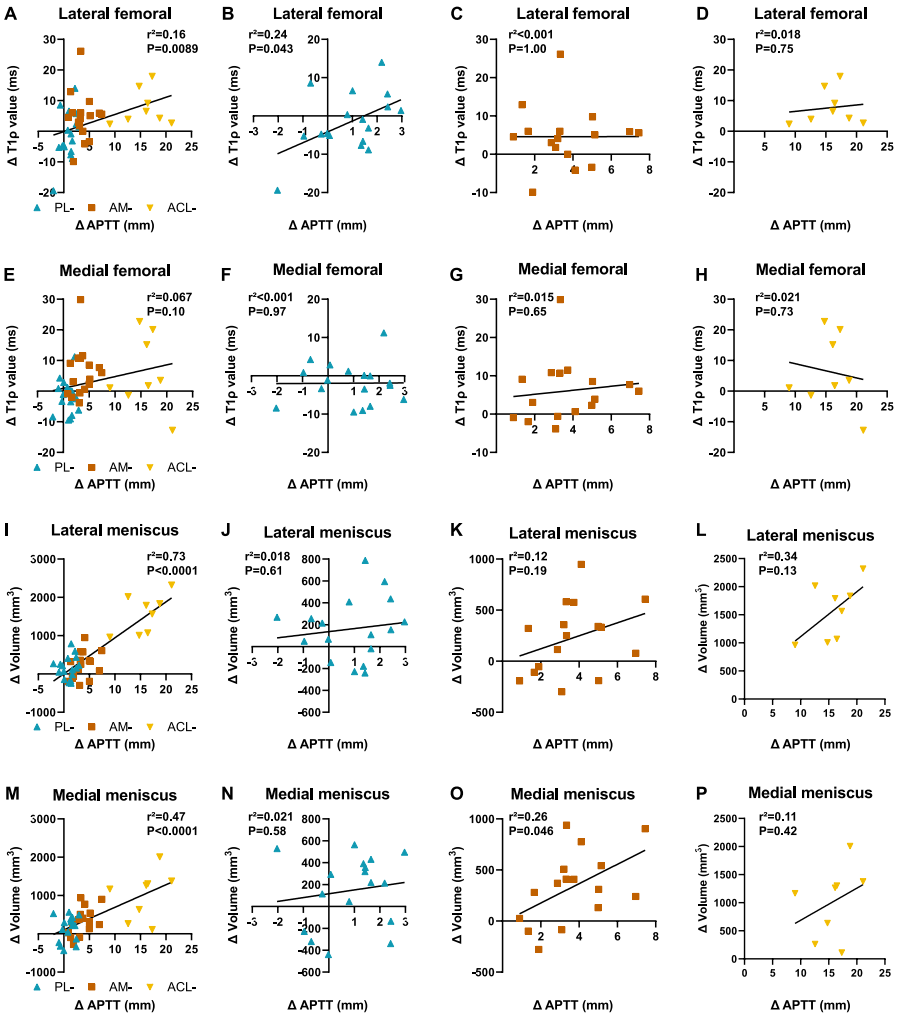

826

827 **Supplementary Fig. 8.** Interlimb difference in (A) lateral and (E) medial femoral cartilage T1rho values and (I)

828 lateral and (M) medial meniscus volumes versus interlimb difference in APTT across all injury groups in pooled

829 juvenile and adolescent pigs. Injury groups separated by PL-, AM-, and ACL- for interlimb differences in (B-D)

830 lateral femoral cartilage T1rho values, (F-H) medial femoral cartilage T1rho values, (J-L) lateral meniscus volume,

831 and (N-P) medial meniscus volume. Statistical results from linear regression analyses shown in graph.

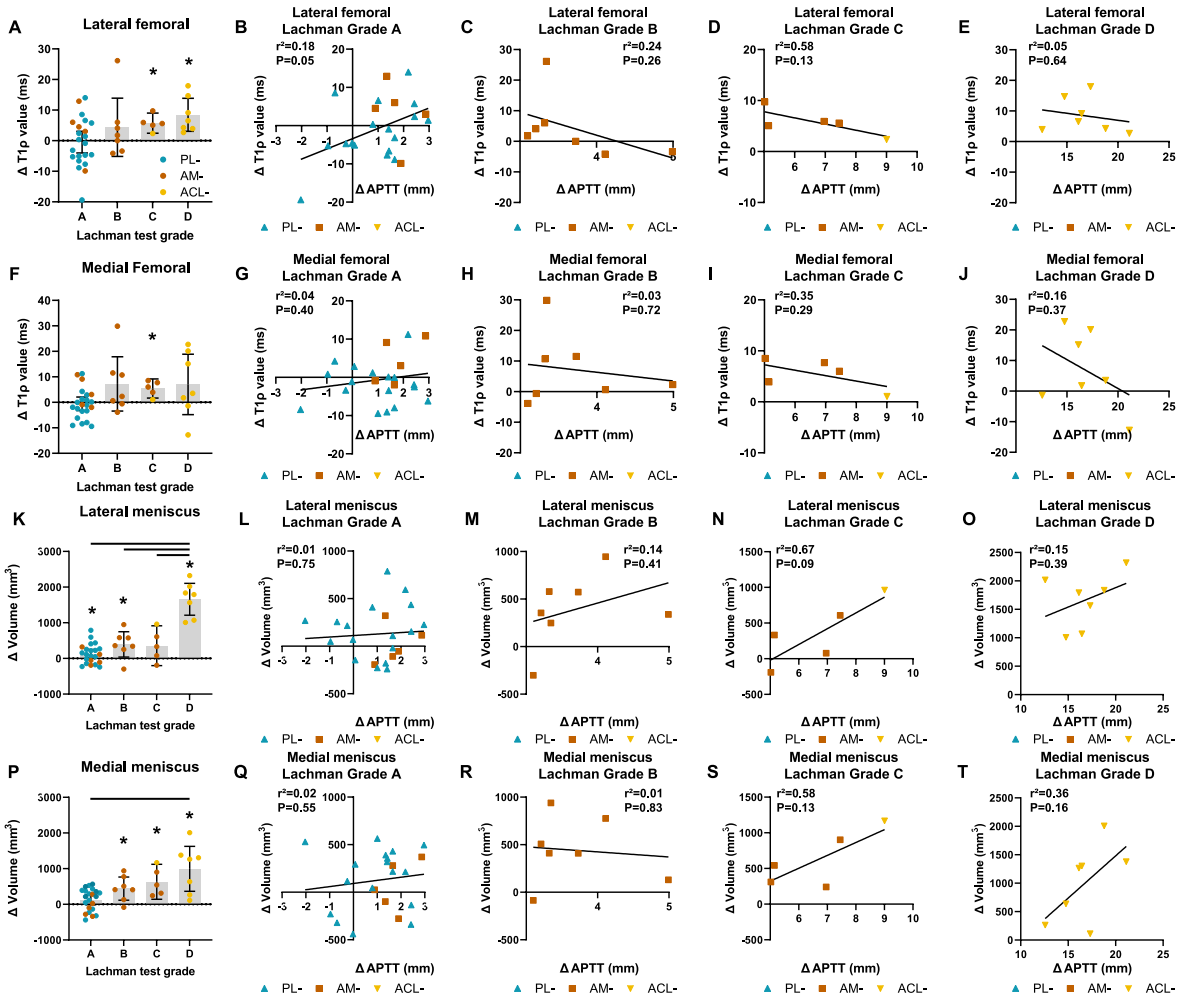

Supplementary Fig. 9. Interlimb difference in (A) lateral and (F) medial femoral cartilage T1rho values and (K) lateral and (P) medial meniscus volumes, grouped by the equivalent Lachman test grade in pooled juvenile and adolescent pigs. *P<0.05 compared to 0 from one sample t-test; bars indicate P<0.05 between injury type, from one-way ANOVA with Tukey post hoc test. Injury groups separated by Lachman grades A-D for interlimb differences in (B-E) lateral femoral cartilage T1rho values, (G-J) medial femoral cartilage T1rho values, (L-O) lateral meniscus volume, and (Q-T) medial meniscus volume. Statistical results from linear regression analyses shown in graph. Individual data points presented with mean ± 95% CI (A,F,K,P).